Exciton related resonant Raman scattering from CdSe quantum dots in an amorphous GeS_2 thin film matrix

2004 J. Phys.: Condens. Matter 16 8221

(http://iopscience.iop.org/0953-8984/16/46/009)

INSTITUTE OF PHYSICS PUBLISHING JOURNAL OF PHYSICS: CONDENSED MATTER

J. Phys.: Condens. Matter **16** (2004) 8221–8232 PII: S0953-8984(04)86043-0

Exciton related resonant Raman scattering from CdSe quantum dots in an amorphous GeS_2 thin film matrix

C Raptis[1,3], D Nesheva[1,2], Y C Boulmetis[1], Z Levi[2] and Z Aneva[2]

[1] Department of Physics, National Technical University of Athens, GR-15780 Athens, Greece
[2] Institute of Solid State Physics, Bulgarian Academy of Sciences, 1784 Sofia, Bulgaria

E-mail: craptis@central.ntua.gr

Received 10 September 2004
Published 5 November 2004
Online at stacks.iop.org/JPhysCM/16/8221
doi:10.1088/0953-8984/16/46/009

Abstract

CdSe quantum dots have been produced in an amorphous GeS_2 thin film matrix by alternating thermal evaporation in vacuum and deposition of several CdSe and GeS_2 layers, with the thickness of the latter being, typically, 20 times larger than that of the former. Raman scattering spectra of these films have been measured over the temperature range 20–293 K using four Ar^+ laser lines for the excitation and studied with emphasis on the position and intensity of the longitudinal optical phonons of CdSe. A shift of these phonons to lower frequencies is seen which increases with decreasing CdSe layer thickness. On the other hand, resonant Raman effects have been observed as the phonon intensity depends strongly on the nominal CdSe layer thickness, excitation energy and temperature. These results imply formation of high quality CdSe quantum dots in the amorphous GeS_2 thin film matrix and are interpreted in terms of *resonant absorption in exciton electronic states of these quantum dots*.

1. Introduction

Low-dimension semiconductors display remarkable size-dependent optical and electronic structure properties [1–8] manifested by band gap variation, spectral tunability of light absorption and emission, confinement induced oscillator strength, etc. Thus, apart from their exciting new physics, they can be used in a number of optoelectronic and non-linear optical applications [9–12]. Nanosize particles, or quantum dots (QDs) as they are often referred to, of various semiconductors have been produced in a variety of large band-gap matrices, such as glasses [1, 4, 6], colloidal solutions [2, 3] and organic or polymeric materials [5, 7] and studied mainly with regard to their emission spectra. On the other hand, semiconductor

[3] Author to whom any correspondence should be addressed.

nanoparticles with narrow-size distribution have been produced in periodic structures, such as amorphous/nanocrystalline multiple quantum wells [13–16].

It is well known that the electron–phonon coupling is of great importance in these materials as its strength increases with decreasing QD size [17] and, because of this, Raman spectroscopy can provide further evidence on such quantum confined structures. Previous Raman investigations [4, 6, 18, 19] on semiconductor QDs embedded in large band-gap matrices have shown a marked shift (up to 8 cm^{-1}) to lower frequencies (red shift) and an asymmetric broadening of the Raman bands, results which are in agreement with the predictions of the phonon localization model [18]. However, for semiconductor nanoparticles formed in multiple quantum wells, it has been found both experimentally [15] and theoretically [18] that the Raman bands sustain a very small red shift ($\sim$1 cm^{-1}), even in the case of superlattices with ultra thin sublayers; clearly, there is a distinction between nanoparticles (QDs) in a matrix and those formed in two-dimensional quantum wells and this should be attributed to the three- and one-dimensional quantum confinement sustained by phonons in the former and latter cases, respectively. Size-dependent resonant Raman scattering has been reported in CdSe [4] and CdS [6] QDs embedded in silicate glasses and in CdSe nanoparticles [15] formed in SiO_x/CdSe multiple quantum wells; the latter results have been interpreted [15] in terms of resonant absorption brought about by an increase of the optical band gap of CdSe with decreasing particle size.

In recent studies [20–22], fabrication of CdSe QDs in a thin film SiO_x matrix has been reported using the multilayer deposition technique; it has been shown [21] that during the deposition of ultra thin layers of thermally evaporated CdSe on relatively 'rough' SiO_x layers, a self-organized formation of CdSe nanoparticles takes place which are distributed in space according to the surface roughness of the oxide layer underneath. It has been proposed [21, 22] that at the start of CdSe layer deposition, the first nuclei for such particles are formed at positions of the SiO_x layer for which the surface curvature and intrinsic stress are greatest, then the following CdSe deposition does not result in the formation of further nuclei, but simply leads to an increase in size of the existing nanoparticles. This proposition has been based on the observation of a rather narrow nanoparticle size distribution in SiO_x–CdSe films [21].

In order to draw further supporting evidence for the above described mechanism of self-organized nanoparticle formation, we have prepared a-GeS_2–CdSe composite thin films in an attempt to produce CdSe QDs in the amorphous matrix of GeS_2. In this study, Raman scattering from such composite films is reported in which the GeS_2 layer thickness is 20 times larger than that of the CdSe ones. Another motivation for this study is to investigate, via the Raman scattering characteristics (position and intensity of Raman bands), the nature and quality (shape, size distribution, etc) of the low-dimension CdSe particles formed in the respective layers. Further, as the studies on QDs to date refer almost exclusively to large band-gap matrices, we extend the studies on low-dimension semiconductors by using a lower band-gap matrix material, namely amorphous semiconducting GeS_2. Temperature dependent Raman measurements have been carried out on a variety of a-GeS_2–CdSe composite films in the range 20–293 K using four exciting laser lines. From the shift of the Raman bands it is concluded that CdSe QDs are formed in the GeS_2 matrix. Resonant Raman scattering is observed and related to light absorption in several excited electronic states of CdSe QDs.

2. Experimental details

Composite a-GeS_2–CdSe thin films were prepared in the shape of almost square platelets ($\sim$1 cm^2 area) by alternating thermal evaporation of GeS_2 and CdSe from two independently heated tantalum crucibles at a vacuum of 10^{-4} Pa and deposition on Corning 7059 glass or

crystalline Si substrates at room temperature [22]. The nominal thickness of a single CdSe layer was $d_{CdSe} = 1, 2, 3$ and 5 nm, while the total thickness of all CdSe layers in each sample was 75–80 nm. All samples had GeS_2 'matrix' layers with a typical thickness of $d_{matrix} = 20\ d_{CdSe}$ (i.e. $d_{matrix} = 20$–100 nm) and the total thickness of all GeS_2 layers amounted to 1500–1600 nm.

Stokes Raman spectra in a pseudo-backscattering geometry were recorded using a system of a SPEX 1403 double monochromator (operated at a spectral slit width of $\sim$3 cm^{-1}) and a cooled photomultiplier connected to photon counting equipment. The 457.9 (2.71), 476.5 (2.60), 488 (2.54) and 514.5 nm (2.41 eV) lines of an Ar^+ laser were used for the excitation in a line focusing configuration (cylindrical lens) in order to avoid degradation of the films. Raman spectra were obtained at several temperatures over the range 20–293 K in vacuum (inside the cryostat) and at 293 K in air, with the laser beam power density being 4 and 8 W mm^{-2} for the measurements in vacuum and air, respectively. A closed cycle He cryostat (20–300 K) was used for the low temperature Raman measurements.

3. Results and discussion

The room temperature Raman spectra of a-GeS_2–CdSe films (having different CdSe layer nominal thickness) excited by the 488 and 514.5 nm laser lines and recorded in air are shown in figures 1 and 2, respectively. For comparison, the Raman spectrum of a pure GeS_2 film is also given in figure 1. The peak at 343 cm^{-1} in the spectra of figures 1 and 2 is the main band of amorphous GeS_2 [23] and its intensity is, within small margins, the same for all films, a result which is anticipated given that the total thickness of GeS_2 layers is equal for all samples and that no significant variation of their optical gap is expected (with d_{matrix}) for such thickness values ($d_{matrix} \geqslant 20$ nm). Hence, in order to compare the Raman scattering intensities from CdSe layers and eliminate any small variations of sample parameters (thickness, surface quality) or measuring conditions, the thin film spectra of each figure 1 and 2 were normalized with respect to the maximum of the 343 cm^{-1} peak of the spectrum of the single layer of pure GeS_2 film. Three more bands observed at 260, 370 and 435 cm^{-1} are also due to amorphous GeS_2 [23]. The band at $\sim$205 cm^{-1} in the spectra of figures 1 and 2 is attributed to scattering from the CdSe layers as it is known [24] that the 1LO Raman phonon of bulk CdSe wurtzite crystal appears at 210 cm^{-1}. The inset of figure 1 shows, in detail, the variation of the 1LO band with d_{CdSe} for the four samples in hand. Further peaks at about 280 and 410 cm^{-1}, appearing in the spectra of films with $d_{CdSe} = 2$ or 3 nm, are discussed below.

The position of the 1LO band depends on the CdSe layer nominal thickness and shifts from about 208 ($d_{CdSe} = 5$ nm) to 204 cm^{-1} ($d_{CdSe} = 1$ nm), an effect illustrated better in the inset of figure 1; also, the band becomes increasingly asymmetric on the low frequency side with decreasing d_{CdSe}. A total shift of up to 6 cm^{-1} is observed in our spectra for the 1LO band in comparison to its single crystal position [24]. This shift is slightly less than the maximum observed in other studies [4, 19] of CdSe QDs embedded in large band-gap silicate matrices. This small difference may be attributed to the different environment of the GeS_2 matrix in which the red shift is partly counter-balanced by a strain-induced blue shift due to a compressive stress by the GeS_2 matrix. Generally, our results are in good agreement with previous studies [4, 6, 18, 19] and imply formation of CdSe QDs which are subjected to a three-dimensional quantum confinement, thus allowing observation of phonon scattering contributions also from points of the Brillouin zone away from its centre, where the optic branches show lower energies [4]. In fact, the Raman results of this work confirm the conclusions of previous electron microscopy [22] and absorption [25] studies on these a-GeS_2–CdSe composite films about the formation of CdSe QDs.

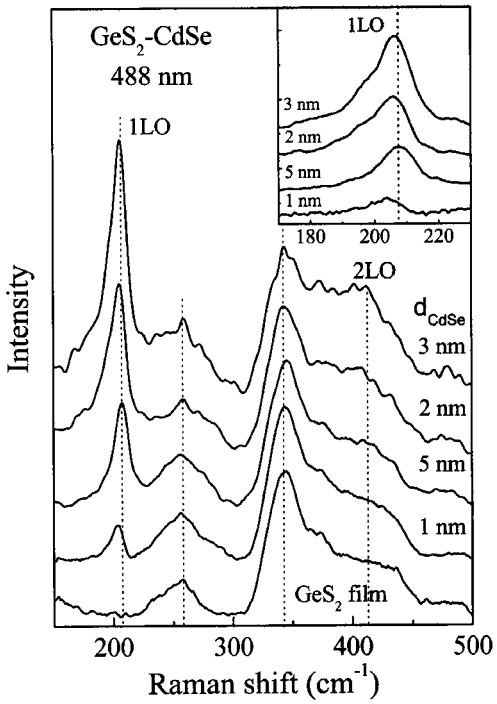

Figure 1. Room temperature Raman scattering spectra of a-GeS_2–CdSe composite films for four values of nominal thickness d_{CdSe} of the CdSe layers and of an amorphous GeS_2 single layer, excited by the 488 nm Ar^+ laser line. The inset shows, in detail, the shift towards the lower frequencies (red-shift) of the 1LO phonon band of CdSe with decreasing d_{CdSe}. All spectra are normalized with respect to the 343 cm^{-1} band of the amorphous GeS_2 matrix.

Furthermore, the spectra of figures 1 and 2 imply that resonance Raman scattering takes place as the intensity of the 1LO band strongly depends on d_{CdSe}; specifically, this band shows maximum intensity for $d_{CdSe} = 3$ (2) nm when excitation is done by the 488 (514.5) nm line. Intensity comparisons between the spectra of figures 1 and 2 show that the resonant effects are stronger when the 514.5 nm line is used for the excitation and this is confirmed by the strong appearance of extra spectral features in the spectra of films with $d_{CdSe} = 2$ or 3 nm (figure 2), namely bands at about 280 and 410 cm^{-1}, corresponding to second order combination (additive) scattering [24, 26]; these bands are weakly observed also when the 488 nm line is used to excite the respective samples (figure 1). In fact, the band at $\sim$410 cm^{-1}, which has also been observed strongly in a previous study [15], is attributed to the 2LO second order band which appears at 420 cm^{-1} in single crystals of CdSe [24, 26]. This second order Raman band is red-shifted in our spectra (figure 2) because of the phonon confinement effect. A similar feature at about 280 cm^{-1} appears in the spectrum of bulk CdSe crystals [24, 26] which has not been assigned, but, because of its broad character should be attributed to combination (addition) of different (TO + LO) optical phonons. These results show that excitation with the 514.5 nm line corresponds to better resonance conditions compared to excitation with the 488 nm line.

In order to draw further evidence on the dependence of the 1LO intensity on the excitation energy, we have also used the 457.9 (2.71) and 476.5 nm (2.6 eV) Ar^+ laser lines for the excitation of Raman spectra of the '2', '3' and '5' nm samples. In figure 3 the spectra of the '3' and '5' nm samples are shown excited by the 476.5, 488 and 514.5 nm lines; the spectra

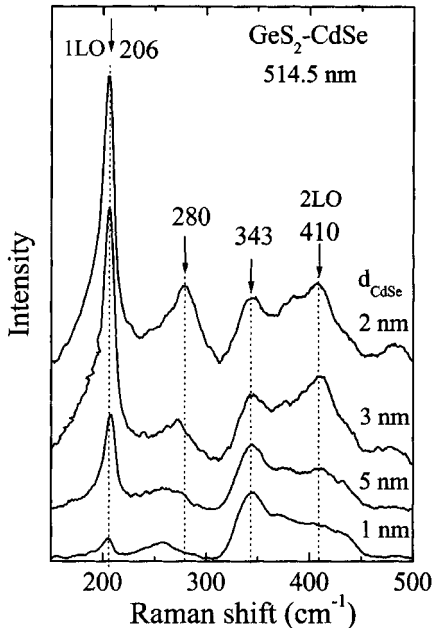

Figure 2. Room temperature Raman scattering spectra of a-GeS_2–CdSe composite films for four values of nominal thickness d_{CdSe} of the CdSe layers, excited by the 514.5 nm Ar^+ laser line. All spectra are normalized to the 343 cm^{-1} band of the amorphous GeS_2 matrix.

have been measured inside the cryostat and are normalized to the 343 cm^{-1} band of GeS_2. The observed intensity variation of the 1LO band with laser energy is very unlikely to be caused by variable absorption by the GeS_2 matrix as it is known [27] that the Raman intensity from pure GeS_2 glass is almost independent of the excitation energy in the range 2.0–2.7 eV. It is, therefore, obvious from figure 3 that the 1LO band is stronger when the 514.5 nm line is used for the excitation and this trend is observed in spite of the ν^4 dependence of the Raman scattering cross-section which favours the blue line excitations. Further evidence about this trend is given in figure 4 which shows the Raman spectrum of the '2' nm sample excited by each of the four laser lines used in this work; each spectrum is normalized first with reference to the ν^4 factor of the respective line and then all four spectra are normalized to the peak of the 343 cm^{-1} band of GeS_2. The normalized, integrated intensity of the 1LO band from the spectra of figure 4 has been plotted against the excitation energy and this plot is given in the inset of figure 4, showing, again, that excitation with the 514.5 nm is closer to resonance.

It is known [28] that in semiconductor QDs with a parabolic dispersion of electron and hole bands, the three-dimensional carrier confinement results in the appearance of a series of discrete levels in both valence and conduction bands. In this simplified parabolic-band model, optical transitions are allowed between electron and hole states of the same symmetry and the QD conduction band is reasonably described by this model [28]. Due to the spin–orbit interaction, the valence band splits into fourfold and twofold degenerate bands and calculations performed taking into account this degeneracy and the valence band mixing in QDs have shown [2, 28, 29] that electronic transitions are allowed between various levels of the valence band and the lowest level of the conduction band ($1S_e$). In this situation, the lowest energy electronic transition $1S_{3/2}$–$1S_e$ defines the optical band gap of CdSe QDs [2, 28, 29]. Besides, as a consequence of the breakdown of selection rules, several distinct bands should appear in the absorption or

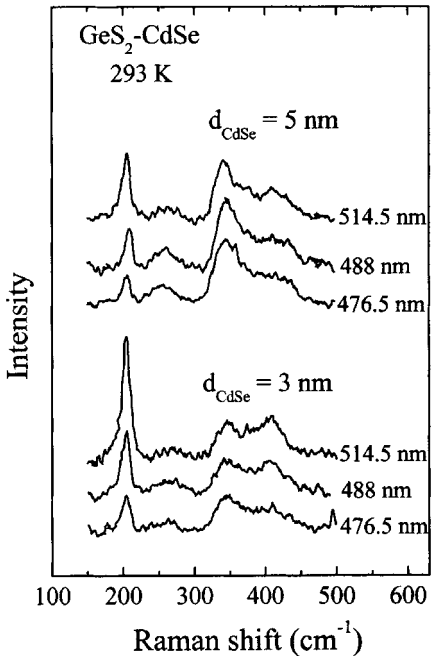

Figure 3. Room temperature Raman scattering spectra of two a-GeS_2–CdSe composite films with CdSe nominal layer thickness of $d_{CdSe} = 3$ and 5 nm, excited by the 488, 514.5 and 476.5 nm Ar^+ laser lines. Each series of spectra correspond almost to the same sample spot and are normalized to the peak intensity of the 343 cm^{-1} band of the amorphous GeS_2 matrix.

photoluminescence excitation (PLE) spectra of high quality (that is, narrow size distribution and small shape variation) CdSe QDs related to the so-called high-energy excitons [2, 28, 29]. Indeed, a number of bands have been observed in the PLE spectrum of colloidal CdSe QDs [2]. However, in absorption spectra of CdSe QDs in amorphous matrices (which display a relative wide size distribution), only two such features have been observed [28, 29] and related to $1S_{3/2}$–$1S_e$ and $2S_{1/2}$–$1S_e$ transitions. Intensity evaluations of PLE results [2] have shown that the observed bands correspond mainly to $n_hS_{3/2}$–$1S_e$, $n_hS_{1/2}$–$1S_e$ and $1P_{3/2}$–$1P_e$ transitions. Recent calculations [30] of the possibility of observing various excitons in CdSe QDs have shown that it is relatively high for the $2S_{1/2}$–$1S_e$ transition (which originates from the split-off valence subband) in comparison with the $2S_{3/2}$–$1S_e$, $1S_{1/2}$–$1S_e$ and $1P_{3/2}$–$1P_e$ transitions.

In an attempt to observe and identify independently excitonic transitions in the CdSe QDs of this study, spectral photocurrent measurements at room temperature have been performed in these composite films and particularly in the samples with $d_{CdSe} = 3$ and 5 nm; a detailed account of these measurements and results have been presented elsewhere [25]. The transition (exciton) energies obtained from the photocurrent spectra [25] of the films having $d_{CdSe} = 3$ and 5 nm are given in table 1, along with the corresponding transition assignments which were deduced in a sequence of increasing energy; also, in the same table, approximate transition energies are given for the film having $d_{CdSe} = 2$ nm, with the procedure of deducing these energies explained below. Using the values of the lowest transition energies, i.e. the experimental bad-gap energies (third column of table 1) and the size dependence of the energy gap of CdSe [28], we have obtained values of 2.5 and 3.3 nm for the average radius R_{av} of CdSe QDs (second column of table 1) in the films with $d_{CdSe} = 3$ and 5 nm, respectively; for the film

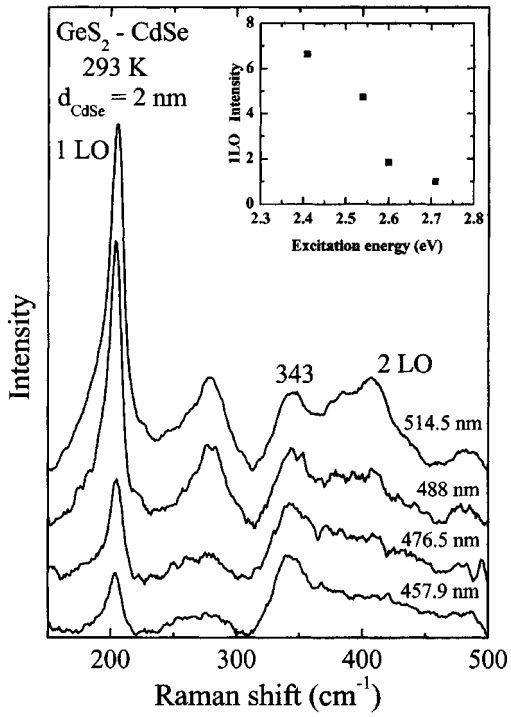

Figure 4. Room temperature Raman scattering spectra of an a-GeS_2–CdSe composite film with CdSe nominal layer thickness of $d_{CdSe} = 2$ nm, excited by the 457.9, 476.5, 488 and 514.5 nm lines. The spectra have been normalized with reference to the excitation energy (i.e. to the ν^4 factor) and then to the peak intensity of the 343 cm^{-1} band of the amorphous GeS_2 matrix. The inset shows the integrated intensity of the 1LO phonon of CdSe plotted against the excitation energy; the integrated intensity is normalized to the respective intensity of the spectrum excited by the 457.9 nm line.

with $d_{CdSe} = 2$ nm, an average QD radius of ∼1.5 nm has been obtained from transmission electron microscopy data [22] which in any case have not given as accurate QD size values as those obtained from the photocurrent measurements. An approximate band-gap energy for QDs of the $d_{CdSe} = 2$ nm film (average QD radius $R_{av} \sim 1.5$ nm) has been estimated from the size dependence [28] of the CdSe band gap.

The estimated QD radii are smaller than the value of 5.6 nm which corresponds to the exciton Bohr radius in CdSe [29] and, hence, a strong confinement regime should be effective for the QDs of this work. Bearing in mind the nominal thickness of the CdSe layers and the obtained values of QD radii, one may calculate the in-plane density of QDs and draw the conclusion that they are very close to one another or even in contact. However, we know from transmission electron micrographs [22] that the CdSe QDs are not disposed in a plane, but they follow the surface morphology and roughness of the GeS_2 matrix below; this means that the QDs are grown at those areas of the GeS_2 layer for which strain becomes maximum (peaks or valleys of the surface, [22]). Thus, QDs are grown in a sublayer whose thickness is, at least, three times greater than the QD diameter [22]. These results imply that strong confinement conditions exist for the QDs of this work. Moreover, we have additional evidence for the existence of strong electronic confinement in the CdSe QDs. The absorption spectra of these samples obtained by various spectral photocurrent methods show a number of absorption maxima [25]. These maxima appear at the energy positions of several excitonic transitions

Table 1. Electronic transitions of CdSe nanocrystals and respective experimental, estimated and theoretical values of transition energies.

Nominal CdSe thickness d_{CdSe} (nm)	Average CdSe QD radius R_{av} (nm)	$1S_{3/2}$–$1S_e$ Optical band gap E_g^0 at 293 K (eV)	$2S_{3/2}$–$1S_e$ (eV)		$1S_{1/2}$–$1S_e$ (eV)		$1P_{3/2}$–$1P_e$ (eV)		$2S_{1/2}$–$1S_e$ (eV)		$3S_{1/2}$–$1S_e$ (eV)	
			293 K	20 K	293 K	20 K	293 K	20 K	293 K	20 K	293 K	20 K
5.0	3.3[a]	1.94[b]			2.09[b]	2.17[f]	2.19[b]	2.27[f]	2.30[b]	2.38[f]		
			1.99[e]		2.09[e]		2.09[e]		2.29[e]			
3.0	2.5[a]	2.05[b]	2.14[b]	2.22[f]	2.25[b]	2.33[f]	2.34[b]	2.42[f]	2.52?[b]			
			2.13[e]		2.25[e]		2.32[e]	2.40[f]	2.47[e]	2.55[f]	2.52[e]	2.60[f]
2.0	∼1.5[c]	∼2.30[d]	2.42[e]		∼2.60[e]		∼2.70[e]					

[a] Estimated values deduced from the size dependence of the optical band-gap E_g^0 [28] (E_g^0 values from the third column have been used).
[b] Room temperature electronic transition energies obtained from the spectral photocurrent measurements of [25].
[c] Approximate value obtained from the high resolution electron micrographs of [22].
[d] Estimated value of E_g^0 deduced from the size dependence of the optical band-gap [28] (the value of 1.5 nm from the second column has been used for the average CdSe nanocrystal radius).
[e] Room temperature theoretical electronic transition energies from [2] (using the effective mass model of [29]).
[f] Low temperature estimated electronic transition energies deduced from the temperature dependence of the optical band-gap $dE/dT \approx 2.9$ meV K^{-1} [31] of bulk CdSe.

of CdSe QDs, thus indicating the existence of three-dimensional carrier confinement in these QDs and a narrow size distribution.

Furthermore, in table 1 theoretical values of exciton transition energies are given for CdSe QDs with average radii 1.5, 2.5 and 3.3 nm, which have been calculated [2] using the effective mass model [29]; these values are in good agreement with experimental ones obtained by the same authors [2] for colloidal CdSe QDs. One can see that for our samples with nominal $d_{CdSe} = 3$ and 5 nm, there is, in general, good agreement between the room temperature transition energies (and the transition assignments) obtained from the photocurrent measurements [25] and the calculated energy values [2] of these transitions. The only noticeable difference between experimental and theoretical values concerns the $2S_{1/2}$–$1S_e$ transition of the '3 nm' sample; however, since the experimental value involves a large margin of error as the relevant feature corresponds to a 'shoulder' in the photocurrent spectrum [25] of this sample, we rely on the calculated data for further considerations about this transition. As was mentioned previously, the estimation of the optical band gap energy of the '2 nm' sample involves large margins of error and so do the theoretical values which correspond to the optical band gap value (table 1). The exciton energies at 20 K (given in separate columns of table 1) have been obtained assuming the same temperature-induced increase of energy for all excitons and applying the temperature dependence of the optical band-gap for bulk CdSe ($dE/dT \approx 2.9$ meV K^{-1} [31]). The good agreement between the theoretical transition energies [2], obtained for an infinite zero-dimensional quantum well, and the experimental ones [25] for CdSe QDs in a GeS_2 matrix (having a relatively narrow band-gap) may be understood if one considers that CdSe is an n-type semiconductor, while GeS_2 is a p-type one. Therefore, a deep well most likely exists which leads to a strong electron confinement.

Now, returning to the room temperature Raman spectra (figures 1 and 2), if we bear in mind that the energies of the three exciting lines (2.41, 2.54 and 2.60 eV) are greater than the band-gap energies (1.94, 2.05 and ∼2.30 eV) of the samples under consideration in table 1, we conclude that the resonance effects observed in these samples should be due to higher excitonic absorption transitions. According to this consideration when the excitation is realized with the 488 nm line (2.54 eV), nearly resonant absorption in the $1S_{1/2}$–$1S_e$ (2.6 eV) and $2S_{1/2}$–$1S_e$

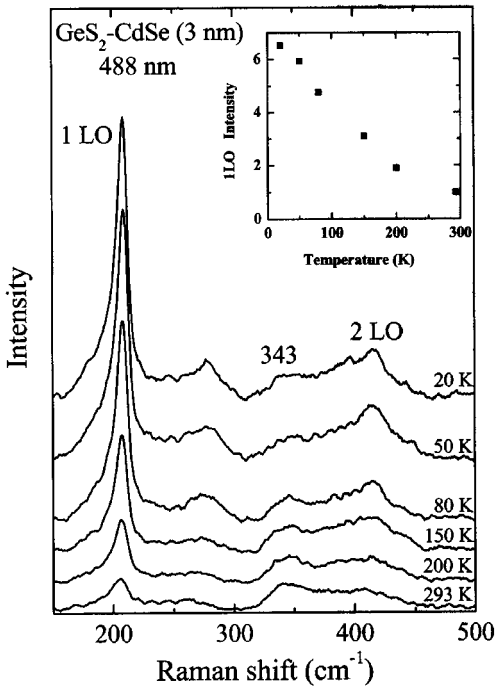

Figure 5. Temperature dependence of the Raman spectrum of an a-GeS_2–CdSe composite film with CdSe nominal layer thickness of $d_{CdSe} = 3$ nm, excited by the 488 nm Ar^+ laser line and over the temperature range 20–293 K. All spectra correspond to the same sample spot and are normalized first to the $n(\omega, T)$ Bose thermal factor and then to the peak intensity of the 343 cm^{-1} band of the amorphous GeS_2 matrix. The inset shows the integrated intensity of the 1LO phonon of CdSe plotted against temperature; the integrated intensity is normalized to the respective intensity of the room temperature spectrum.

(2.47 eV) electronic transitions should be expected for the $d_{CdSe} = 2$ and 3 nm samples, respectively. The two cases are almost equally distant from resonance conditions (by 0.06 and 0.07 eV, respectively), but the probability of the $2S_{1/2}$–$1S_e$ transition is higher than the $1S_{1/2}$–$1S_e$ one [30]. Indeed, maximum intensity for the 1LO Raman band is observed when the $d_{CdSe} = 3$ nm sample is excited by the 488 nm line (figure 1). On the other hand, when the 514.5 nm (2.41 eV) line is used for the excitation, resonant absorption should occur along the $2S_{3/2}$–$1S_e$ ($d_{CdSe} = 2$ nm) and $1P_{3/2}$–$1P_e$ ($d_{CdSe} = 3$ nm) excitons, with the former case expected to be closer to resonance, a result confirmed by the maximum intensity of the 1LO phonon displayed in the Raman spectrum of the $d_{CdSe} = 2$ nm sample (figure 2). In both Raman spectra of the $d_{CdSe} = 5$ nm sample (figures 1 and 2), the 1LO phonon is relatively weak in comparison to those of the $d_{CdSe} = 2$ or 3 nm samples; this is most likely because the exciting laser energies are higher than the energies of all room temperature exciton transitions observed in this sample [25] (see also table 1). Finally, the spectra of the $d_{CdSe} = 1$ nm sample show very weak intensities for the 1LO phonon with either 488 or 514.5 nm line excitation, which is a compatible result bearing in mind that the electronic transition energies of QDs in this sample are expected to be significantly higher than the excitation energies.

Further evidence for the above conclusions has been obtained by measuring the Raman spectra of the $d_{CdSe} = 3$ nm film at several temperatures over the range 20–293 K using the 488, 514.5 and 476.5 nm lines (figures 5–7, respectively). After baseline subtraction, these spectra

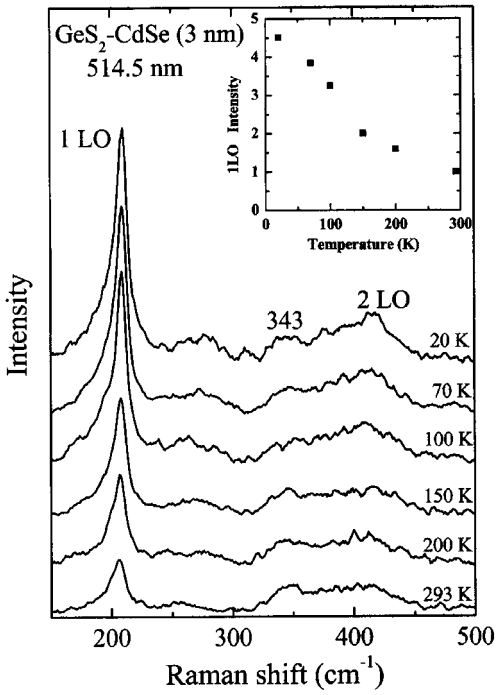

Figure 6. Temperature dependence of the Raman spectrum of an a-GeS_2–CdSe composite film with CdSe nominal layer thickness of $d_{CdSe} = 3$ nm, excited by the 514.5 nm Ar^+ laser line and over the temperature range 20–293 K. All spectra correspond to the same sample spot and are normalized first to the $n(\omega, T)$ Bose thermal factor and then to the peak intensity of the 343 cm^{-1} band of the amorphous GeS_2 matrix. The inset shows the integrated intensity of the 1LO phonon of CdSe plotted against temperature; the integrated intensity is normalized to the respective intensity of the room temperature spectrum.

have been normalized first according to the Bose thermal factor $n(\omega, T)$ and then to the peak of the 343 cm^{-1} band of GeS_2 at room temperature; the latter normalization minimizes any effects of variable absorption by the GeS_2 matrix layers because of an anticipated blue shift of the absorption edge of the layers at low temperatures. Following these normalizations, the integrated intensity of the 1LO band has been plotted against temperature for each excitation and the resulting plots are shown as insets in figures 5–7. The combination of the '3' nm sample and the above mentioned lines results, most likely, in the tuning of the $2S_{1/2}$–$1S_e$ (which has the highest probability [30]), $1P_{3/2}$–$1P_e$ and $3S_{1/2}$–$1S_e$ excitonic transitions, respectively (see table 1). Excitation with the deep blue line (457.9 nm) did not produce noticeable resonance effects most likely because the anticipated higher order (>2.70 eV) transitions have, in general, a lower probability [30]. In these additional experiments, by increasing the exciton energies at low temperatures, we can see whether we move closer to or further away from resonance conditions. A continuous, gradual increase of the 1LO phonon intensity observed with decreasing temperature (figure 5) clearly indicates that the QD absorption approaches near resonance conditions for the predicted $2S_{1/2}$–$1S_e$ excitation at 20 K as the theoretical value of the transition energy (2.55 eV, table 1) becomes comparable to the exciting laser energy (2.54 eV). As was mentioned above, the experimental value (2.52 eV) of the transition energy, obtained by photocurrent measurements at room temperature, is not reliable. Also, compared to the room temperature situation, better resonance conditions should be attained for the $d_{CdSe} = 3$ nm film close to 20 K when excited by the 514.5 nm line as the $1P_{3/2}$–$1P_e$

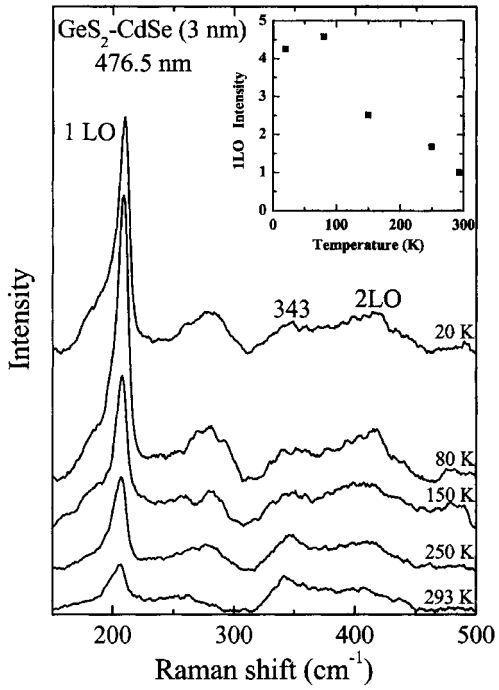

Figure 7. Temperature dependence of the Raman spectrum of an a-GeS_2–CdSe composite film with CdSe nominal layer thickness of $d_{CdSe} = 3$ nm, excited by the 476.5 nm Ar^+ laser line and over the temperature range 20–293 K. All spectra correspond to the same sample spot and are normalized first to the $n(\omega, T)$ Bose thermal factor and then to the peak intensity of the 343 cm^{-1} band of the amorphous GeS_2 matrix. The inset shows the integrated intensity of the 1LO phonon of CdSe plotted against temperature; the integrated intensity is normalized to the respective intensity of the room temperature spectrum and displays a resonance maximum at about 80 K.

exciton energy (2.42 eV, table 1) for this film almost coincides with the laser energy (2.41 eV); indeed, figure 6 shows that the 1LO intensity attains its highest value at 20 K. Finally, when the $d_{CdSe} = 3$ nm sample is excited by the 476.5 nm (2.60 eV) line a resonance peak appears to occur at about 80 K (figure 7) which, according to the expected temperature dependence [31] for the higher order exciton transition $3S_{1/2}$–$1S_e$ (table 1), corresponds to a transition energy of ∼2.58 eV.

The results of figures 4–7 provide further support for the experimental, theoretical and estimated electronic transition energies and the assignments presented in table 1. In addition, this study has shown that resonant Raman scattering can provide valuable information on the quality (nanoparticle shape and size distribution) of low-dimension semiconductor films and structures.

4. Conclusions

Raman scattering spectra have been presented of composite a-GeS_2–CdSe thin films in which the nominal thickness of CdSe layers varies between 1 and 5 nm and the GeS_2 layers are ∼20 times thicker than the CdSe ones. From the red-shift of the 1LO and 2LO Raman bands of CdSe, it is concluded that CdSe quantum dots are formed in the matrix of amorphous GeS_2, a result which confirms previous studies [22, 25] on these films. Resonant Raman effects have been observed in the spectra of films with a CdSe layer thickness of 2 and 3 nm when excited

by the 488 and 514.5 nm Ar^+ laser lines at room temperature and have been related to *resonant light absorption in several exciton transitions of the CdSe quantum dots*. These results have been strongly supported by temperature-dependent Raman measurements in the range 20–293 K and by using a higher energy excitation radiation, namely the 476.5 nm Ar^+ laser line. The results of the present study imply a successful fabrication of CdSe quantum dots in an amorphous GeS_2 matrix and provide further support for the proposed mechanism [21, 22] of self-organized nanoparticle formation on a rough amorphous surface. Also, this work provides convincing arguments that Raman spectroscopy can be successfully applied for the study of the electronic structure of semiconductor quantum dots.

Acknowledgments

DN wishes to thank the National Technical University of Athens (NTUA) for supporting a scientific visit to the Department of Physics of NTUA during which the Raman scattering measurements were carried out. This work was partially supported by the Bulgarian Ministry of Education and Science under grant F-1306.

References

[1] Rodrigues P A M, Tamulaitis G, Yu P Y and Risbud S H 1995 *Solid State Commun.* **94** 583
[2] Norris D J and Bawendi M 1996 *Phys. Rev.* B **53** 16338
[3] Norris D J, Efros A L, Rosen M and Bawendi M G 1996 *Phys. Rev.* B **53** 16347
[4] Saviot L, Champagnon B, Duval E, Kudriavtsev I A and Ekimov A I 1998 *J. Non-Cryst. Solids* **197** 238
[5] Kuno M, Lee J K, Dabbousi B O, Mikulec F V and Bawendi M G 1997 *J. Chem. Phys.* **106** 9869
[6] Saviot L, Champagnon B, Duval E and Ekimov A I 1998 *Phys. Rev.* B **57** 341
[7] Ginger G S, Dhoot A S, Finlayson C E and Greenham N C 2000 *Appl. Phys. Lett.* **77** 2816
[8] Li L S, Hu J T, Yang W D and Alivisatos A P 2001 *Nano Lett.* **1** 349
[9] Brus L E 1991 *Appl. Phys.* A **53** 465
[10] Yoffe A D 1993 *Adv. Phys.* **42** 172
[11] Alivisatos A P 1998 *MRS Bull.* **23** 18
[12] Grätzel M 2000 *Handbook of Nanostructured Materials and Nanotechnology* vol 3, ed H S Nalwa (New York: Academic) p 527
[13] Wu X L, Tong S, Liu X N, Bao X M, Yang S S, Feng D and Siu G G 1997 *Appl. Phys. Lett.* **70** 838
[14] Zacharias M and Streitenberger P 2000 *Phys. Rev.* B **62** 8391
[15] Nesheva D, Raptis C and Levi Z 1998 *Phys. Rev.* B **58** 7913
[16] Nesheva D 2003 *Encyclopedia of Nanoscience and Nanotechnology* ed H S Nalwa (Stevenson Ranch, CA: American Scientific Publishers) p 105 and references therein
[17] Schmitt-Rink S, Miller D A and Chemla D S 1987 *Phys. Rev.* B **35** 8113
[18] Campbell I H and Fauchet P M 1986 *Solid State Commun.* **58** 739
[19] Hwang Y-N, Shin S, Park H L, Park S-H and Kim Y 1996 *Phys. Rev.* B **54** 15120
[20] Nesheva D and Levi Z 1997 *Semicond. Sci. Technol.* **12** 1319
[21] Nesheva D and Hofmeister H 2000 *Solid State Commun.* **114** 511
[22] Nesheva D, Hofmeister H, Levi Z and Aneva Z 2002 *Vacuum* **65** 109
[23] Kotsalas I P and Raptis C 2001 *Phys. Rev.* B **64** 12510 and references therein
[24] Plotnichenko V G, Mityagin Yu A and Vodopyanov L K 1977 *Sov. Phys.—Solid State* **19** 1584
[25] Nesheva D, Levi Z, Aneva Z, Zrinscak I, Main C and Reynolds S 2002 *J. Nanosci. Nanotechnol.* **2** 645
[26] Chang R K, Ralston J M and Keating D E 1969 *Light Scattering Spectra of Solids* ed G B Wright (New York: Springer) p 369
[27] Yamaguchi M, Shibata T and Tanaka Ke 1998 *J. Non-Cryst. Solids* **232–234** 715
[28] Klimov V I 2000 *Handbook of Nanostructured Materials and Nanotechnology* vol 4, ed H S Nalwa (New York: Academic) p 451
[29] Ekimov A I, Hache F, Schann-Klein M C, Ricard D, Flytzanis C, Kudryavtsev I A, Yazeva T V, Rodina A V and Efros Al L 1993 *J. Opt. Soc. Am.* B **10** 100
[30] Laheld U E H and Einevoll G T 1997 *Phys. Rev.* B **55** 5184
[31] Landolt–Bornstein 1982 *Numerical Data and Functional Relationships in Science and Technology* (*Landolt–Bornstein New Series* vol 17b) ed K-H Hellewege (Berlin: Springer) p 203